



HAL
open science

Amide solvent protection analysis demonstrate that amyloid-beta(1-40) and amyloid-beta(1-42) form different fibrillar structures under identical conditions

Anders Olofsson, Malin Lindhagen-Persson, A. Elisabeth Sauer-Eriksson,
Anders Öhman

► **To cite this version:**

Anders Olofsson, Malin Lindhagen-Persson, A. Elisabeth Sauer-Eriksson, Anders Öhman. Amide solvent protection analysis demonstrate that amyloid-beta(1-40) and amyloid-beta(1-42) form different fibrillar structures under identical conditions. *Biochemical Journal*, 2007, 404 (1), pp.63-70. 10.1042/BJ20061561 . hal-00478686

HAL Id: hal-00478686

<https://hal.science/hal-00478686>

Submitted on 30 Apr 2010

HAL is a multi-disciplinary open access archive for the deposit and dissemination of scientific research documents, whether they are published or not. The documents may come from teaching and research institutions in France or abroad, or from public or private research centers.

L'archive ouverte pluridisciplinaire **HAL**, est destinée au dépôt et à la diffusion de documents scientifiques de niveau recherche, publiés ou non, émanant des établissements d'enseignement et de recherche français ou étrangers, des laboratoires publics ou privés.

Amide solvent protection analysis demonstrates that Amyloid- β (1-40) and Amyloid- β (1-42) form different fibrillar structures under identical conditions.

Anders Olofsson^{*}, Malin Lindhagen-Persson, A. Elisabeth Sauer-Eriksson and
Anders Öhman^{*}

Umeå Centre for Molecular Pathogenesis, Umeå University, SE-901 87 Umeå, Sweden.

^{*}Corresponding authors.

Full address for correspondence:

Anders Öhman/Anders Olofsson

Umeå Centre for Molecular Pathogenesis

Umeå University

SE-901 87 Umeå

Sweden

E-mail: anders.ohman@ucmp.umu.se, anders.olofsson@ucmp.umu.se

Tel.: +46 (0)90 785 6737, +46 (0)90 785 6796

Fax.: +46 (0)90 77 80 07

Running title: NMR analysis of A β (1-40) amyloid.

Keywords: Alzheimer's disease, Amyloid- β peptide, NMR, AFM, H/D exchange.

Alzheimer's disease (AD) is a neurodegenerative disorder characterized by self-assembly and amyloid formation of the 39-43 residue long Amyloid- β (A β) peptide. The most abundant species, A β (1-40) and A β (1-42), are both present within senile plaques, but A β (1-42) peptides are considerably more prone to self-aggregation and are also essential for the development of AD. To understand the molecular and pathological mechanisms behind AD, a detailed knowledge of the amyloid structures of A β -peptides is vital. In the present work we have used quenched hydrogen/deuterium exchange NMR experiments to probe the structure of A β (1-40) fibrils. The fibrils were prepared and analyzed identically as in our previous study on A β (1-42) fibrils, allowing a direct comparison of the two fibrillar structures. The solvent protection pattern of A β (1-40) fibrils revealed two well protected regions, consistent with a structural arrangement of two β -strands connected with a bend. This protection pattern partly resembles the pattern found in A β (1-42) fibrils, but the A β (1-40) fibrils display a significantly increased protection for the N-terminal residues Phe4-His14, suggesting that additional secondary structure is formed in this region. In contrast, the C-terminal residues Gly37-Val40 show a reduced protection that suggests a loss of secondary structure in this region and an altered filament assembly. The differences between our study and other similar investigations suggest that subtle variations in fibril-preparation conditions may significantly affect the fibrillar architecture.

INTRODUCTION

Self-assembly and deposition of proteins into amyloid fibrils and plaques are phenomena that currently have been linked to around 20 different human diseases [1]. The long unbranched fibrils that constitute amyloid typically have a diameter between 50-130 Å and a characteristic cross- β pattern in which β -strands are arranged perpendicular to the fibrillar axis [2-5]. The best known example of such a disorder is Alzheimers disease (AD)¹, which is correlated with the aggregation of an endogenic peptide denoted Amyloid β (A β)-peptide [6-12]. The A β -peptide is a result of proteolytic processing of the membrane-bound amyloid precursor protein. This excision generates an ensemble of peptides with various lengths, where each species exhibits rather distinct biophysical properties. The clinically most relevant fragments include 39-43 residues, of which the A β (1-40) and A β (1-42) peptides are

¹The abbreviations used are: AD, Alzheimer's disease; A β , Amyloid- β ; NMR, nuclear magnetic resonance; H/D, hydrogen/deuterium; AFM, atomic force microscopy.

the most abundant [13]. Although the ratio between A β (1-40) and A β (1-42) peptides in the human body is about 7:1, the A β (1-42) variant is overrepresented in senile plaques, and also present in the first deposits found during disease development [14, 15]. Overproduction of A β (1-42) has moreover been linked to early onset of AD [16, 17] and recent experiments in a AD mouse-model suggest that selective inhibition of the A β (1-42) variant abolishes the disease [18]. Although the cytotoxic mechanism *in vivo* is not completely understood at present the correlation with aggregation of the A β -peptide is convincing [6-11]. One potential therapeutic approach hence involves design of inhibitors of the A β -assembly. Therefore, a thorough knowledge about the molecular architecture of the fibrillar states of A β peptides is necessary. In particular, it is of interest to compare the structure of the more aggregation prone A β (1-42) variant with its shorter counterparts.

Structural studies of amyloid are hampered by its non-crystalline and solid nature where conventional methods using crystal diffraction and liquid nuclear magnetic resonance (NMR) cannot be readily employed. An alternative technique is solid-state NMR, a method that has been used extensively to successfully investigate the structure of fibrils from A β (10-35), A β (1-40) and A β (1-42) peptides [19-24]. More recently, the combined use of quenched hydrogen/deuterium (H/D) exchange and solution NMR spectroscopy has proven extremely valuable for studies of the structural and dynamical properties of amyloid fibrils [25-31], including fibrils from both the A β (1-40) and A β (1-42) variants [26, 30, 31]. With this method, identification of the core region of a fibril is possible since the secondary structure and solvent exclusion in the core protect the labile amide protons from exchanging with the surrounding deuterons. After a designated incubation time in D₂O the solvent protection is trapped via a rapid conversion of the fibrils into a monomeric and NMR-detectable state during conditions of low back-exchange. By following the post-trap decay of the H/D exchange the method pinpoints the fibrillar core in a residue-specific and quantitative manner. Applying this method to A β (1-42) fibrils we previously identified two solvent-protected core regions, comprising residues Glu11-Gly25 and Lys28-Ala42 [26, 30, 31]. The residues in-between, Ser26 and Asn27, as well as the very N-terminal residues, Asp1-Tyr10, were solvent accessible. These findings agree well with the most recent fibrillar models derived from solid-state NMR data [23, 24], but differ somewhat from similar H/D exchange NMR studies [26, 30, 31]. Detailed comparisons of the various studies on A β -fibrils are however complex, since recent quenched H/D exchange NMR and solid-state NMR data

indicate that rather subtle changes in fibril-growth conditions significantly affect the fibrillar structure.

In order to identify discriminating features between A β (1-40) and A β (1-42) fibrils, we have performed quenched H/D exchange NMR on A β (1-40) fibrils prepared under conditions identical to the ones used in our investigation on the A β (1-42) fibrils [31]. Two highly protected core regions were identified in good agreement with our results for the A β (1-42) fibrils. However, a significantly higher protection of the N-terminal region, as well as a reduced solvent protection for the C-terminal residues, discriminate the A β (1-40) from the A β (1-42) fibrillar structure and provide new structural data for current models of A β architecture.

EXPERIMENTAL

NMR Spectroscopy and Resonance Assignment of A β (1-40)

Isotope-enriched chemicals were purchased from Cambridge Isotope Laboratories, USA. Uniformly ^{15}N -labeled A β (1-40) was obtained from Alexo-Tech, Umeå, Sweden (www.alexo-tech.com). The NMR sample used for resonance assignment contained ~2 mM recombinant A β (1-40) and was prepared in 80% 1,1,1,3,3,3-Hexafluoroisopropanol-D₂ (HFIP)/20% H₂O, 150 mM NaCl at pH 3.0, as previously described [31]. Homonuclear 2D clean-TOCSY and heteronuclear 2D ^{15}N -HSQC, as well as 3D ^{15}N -DIPSI-HSQC and ^{15}N -NOESY-HSQC experiments were collected at 15°C on a 600 MHz Bruker AVANCE spectrometer, equipped with a 5-mm triple-resonance, pulsed-field z-gradient cryoprobe. Recorded experiments were processed using NMRPipe [32] and the sequence-specific backbone resonance assignment was determined with Ansig for Windows [33].

H/D Exchange of A β (1-40) Fibrils

The fibril samples for the H/D exchange experiments were produced, treated, and analyzed by NMR in a manner identical to our previous work on A β (1-42) fibrils [31]. Briefly, fibrils were grown by incubating a sample of 1 mM ^{15}N -labeled A β (1-40) in 5 mM phosphate buffer pH 7.0 and 50 mM NaCl, and incubated at 37°C for 5-8 days with agitation at 130 rpm. Immediately after dissolution and prior to fibril formation the peptide displays a circular dichroism spectrum characteristic for a primarily random coil conformation (data not shown). The fibril solution was divided into three aliquots and the pellets were recovered by short centrifugations at 13000g. The H/D exchange was initiated by diluting the pellets 30 times

using a D₂O-solution and 50 mM NaCl, pH 7.0. The fibrils were recovered through centrifugation and the washing procedure repeated once to remove residual H₂O and soluble material. Two of the aliquots were subsequently incubated in D₂O for 2 and 24 hours, respectively, including the period for the buffer exchange procedure. The third aliquot contained fully protonated fibrils and served as a control, to discriminate between rapid exchange as a result of the experimental procedure and exchange as a result of the preceding incubation in D₂O. At the end of the incubation period the fibrils in all three fibril samples were rapidly converted into NMR-detectable monomers as described in [31], in 80% HFIP/20% D₂O, 150 mM NaCl, pD 2.6, a solution known to induce a significant fraction of α -helicity in A β -peptides [34]. Each sample acquired a peptide concentration corresponding to approximately 2 mM of monomeric A β (1-40). Hydrogen exchange was subsequently monitored by recording series of heteronuclear 2D ¹⁵N-HSQC experiments, typically started 6-8 minutes after fibril dissolution. The acquisition time for each ¹⁵N-HSQC experiment was 10 minutes using four transients per increment and 128 (t₁) x 1024 (t₂) complex data points. Prior to each ¹⁵N-HSQC experiment a 1D proton NMR spectrum was recorded to quantitatively monitor the dissolution of fibrils into monomers.

Data Analysis and Structural Modeling

Processing and analysis of 1D experiments were carried out in TOPSPIN (Bruker Biospin), while processing of the recorded ¹⁵N-HSQC-experiment was performed in NMRPipe [32]. Peak volumes in baseline-corrected ¹⁵N-HSQC experiments were determined using NMRView software routines [35]. The non-exchangeable methyl region in the recorded series of 1D spectra was integrated and fitted to a single exponential function to determine the relative monomer concentration of the samples and the rates of fibril dissolution. This was taken into account when the intensities of individual amide resonances in the series of ¹⁵N-HSQC spectra were fitted to a single exponential decay in the software Grace. By extrapolating the intensities to time zero the signal intensity in the fibrillar state was obtained. Residue-specific protection ratios were determined from the signal intensity ratio of a sample pre-incubated in D₂O and the fully protonated control. The experimental uncertainty of the protection ratios were determined by propagation of errors using the standard deviations of the fitted exponentials. It is important to stress the significance of analyzing the decay of the fully protonated control as this makes it possible to discriminate between exchanging protons in the fibrillar and monomeric state. A detailed description of the analysis procedure is found

in our previous study on A β (1-42) [31]. Protection ratios were mapped onto a model of the fibrillar structure of A β (1-40) by using MOLMOL [36]. This model was prepared from the coordinates of the recent solid-state NMR model of the A β (9-40) fibril, kindly provided by Dr. Robert Tycko [19], to which the missing N-terminal residues were added from the coordinates of a structure of A β (1-16) (PDB code: 1ZE7) [37]. From this new A β (1-40) fibrillar model, a model of a A β (1-42) fibril was generated by adding the two additional C-terminal residues from our previous A β (1-42) model [31] and by placing the two filaments in a recently proposed shifted arrangement [24]. Details about various fibrillar models are described further in the Discussion section. Modifications and energy minimization of the models were performed in MOLMOL [36] and Swiss-PdbViewer [38].

Atomic Force Microscopy (AFM)

A portion of the A β (1-40) fibril solution was diluted in 10 mM phosphate buffer, pH 7.0, and 50 mM NaCl, to approximately 5 μ M peptide solution that was applied onto freshly cleaved ruby red mica (Goodfellow, Cambridge, UK). The solution was allowed to adsorb for 30 s, followed by washing with distilled water three times and air drying. Analysis was performed using a Nanoscope IIIa multimode AFM (Digital Instruments Santa Barbara, USA) in tapping ModeTM in air. A silicon probe was oscillated at around 280 kHz, and images were collected at an optimized scan rate corresponding to one Hz. The images were flattened and presented in amplitude mode using Nanoscope software (Digital Instruments).

RESULTS

Sequence Specific Backbone Assignment of A β (1-40) Monomers in Solution

The recorded spectra were of high quality with good dispersion and few overlapping resonances. The sequence-specific backbone resonance assignment was determined from the NOESY spectrum via a sequential walk between backbone amide resonances and via characteristic α -helical sequential or medium-range NOE resonances. All of the 39 backbone amide resonances (residues 2-40) could be identified and only two of these, Asn27 and Ile32, showed significant overlap. This ambiguity, however, does not affect the analysis of the H/D exchange as discussed below. Overall the assignment agreed extremely well with our assignments for A β (1-42) [31], and chemical shift differences were mainly detected in the C-terminal region of the peptides.

Fibril Formation and AFM Analysis of A β (1-40)

Fibrils were formed by incubating a sample containing 1 mM ^{15}N -labelled A β (1-40) peptide in 5 mM phosphate buffer, pH 7.0 and 50 mM NaCl, for 5-8 days at 37°C with agitation at 130 rpm. The peptide solution acquired a gel-like appearance and the presence of fibrils was verified by AFM (Figure 1A). The fibrils were of varying length, 100-500 nm, with a height of 3.5-7 nm and smooth morphology.

Determination of Protection Ratios of A β (1-40) Fibrils

Fibrillar material was collected by centrifugation and H/D-exchange was carried out by resuspension and incubation of the fibrillar pellets in D₂O. The conversion of fibrils into NMR-detectable monomers followed a single exponential function with an average rate constant of 0.0028 min⁻¹. More than 91% of the total fibril material was dissolved prior to the first ^{15}N -HSQC spectrum. A spectrum of the fully protonated peptide is shown in Figure 2A and spectra of D₂O exchanged fibrils, recorded 11 and 203 minutes after fibril dissolution, are shown in Figures 2B and C, respectively. Analysis of the control sample showed that 36 out of 39 amide resonances could be used as probes for determining the solvent protection of the fibril. Residues Ala2 and Asp7 experience a post-trap exchange rate which is too fast for detection. The minute protection observed for Glu3 is too small and decays too fast to permit a reliable fit. Post-trap decays and curve-fits for five residues, Gln15, Phe20, Val24, Met35 and Val36, are shown in Figure 3.

The solvent protection patterns for fibrils that were pre-incubated in D₂O for 2 or 24 hours are shown in Figure 4A. A total of 35 residues were protected and the protection ratio in general decreased with exchange time, 66% and 60% overall ratio at 2 and 24 hours, respectively. Two well-protected bell-shaped regions were identified covering residues Ser8-Gly25 and Gly27-Val40, with the strongest protection (close to 90%) for residues Leu17-Gly25 and Ala30-Val36. Notably, Phe4 and Arg5 are partially protected, His6 is unprotected, and Ser26, Gly38 and Val39 are quite poorly protected. Since Asn27 and Ile32 are overlapping, the signal decay rate had to be fitted to a bi-exponential function. Their decay rates were unambiguously assigned through comparisons with the decay rates for these residues in our A β (1-42) study [31] and in H/D exchange NMR experiments performed on A β (1-40) under slightly different solvent conditions where these resonances were not overlapping (data not shown). The protection ratio determined for Asn27 is less accurate since it has lower signal intensity and much faster exchange rate than Ile32 (0.0318 compared

to 0.0008 min^{-1}). Fast amide proton exchange rates within the monomeric structure are also the origin of experimental uncertainties of the fibrillar protection ratios. Figure 4B shows the fibrillar solvent protection pattern for A β (1-42), where 35 out of 41 residues were useful as probes. The remaining six residues (Ala2, His6, Asp7, Ser8, His14 and Asp23) experience exchange rates in the monomeric state, which prevent detection [31].

DISCUSSION

The structural organization of fibrils from either A β (1-40) or A β (1-42) peptides have been extensively investigated, resulting in several proposed models all with a characteristic cross- β structure (reviewed in [39, 40]). Solid-state NMR studies on A β fibrils have significantly contributed to the understanding of the fibril architecture, and suggest a fibrillar model in which the A β -peptide attains two β -strands that stack perpendicular to the fibrillar axis, forming a filament structure of two separate in-register parallel β -sheets [21, 22]. Scanning transmission electron microscopy in combination with solid-state NMR studies furthermore suggests that the smallest fibrillar form under physiological conditions includes two filaments [21] arranged in an anti-parallel fashion [23, 24]. Fibril cross-sections describing the suggested molecular structures as well as the filament arrangements for A β (1-40) and A β (1-42) fibrils, respectively, are schematically shown in Figure 5A and B. Two alternative models have also been described; the A β (1-40) fibril model shown in Figure 5C derived through scanning cysteine mutagenesis and threading analysis [41], and the A β (1-42) fibril model shown in Figure 5D derived from double compensatory mutagenesis in combination with H/D exchange NMR [30]. Although most of the recently presented structural information on A β -fibrils is similar, it is increasingly evident that minor alterations of the solvent conditions and procedure for fibril preparation have significant impact on the corresponding structures. Interestingly a recent study clearly establishes a correlation between A β -fibrillar structure and neurotoxicity [9]. This observation may in part explain previously diverging results for A β toxicity, and it highlights the need for further structural studies. The substantial differences between A β (1-40) and A β (1-42) with regard to their aggregation propensity and role in AD pathology make it important to identify structural discrepancies in their fibrillar forms. Previous studies are difficult to compare since different fibril growth conditions were used.

In the present study we have determined the solvent protection pattern of fibrils from A β (1-40), see Figure 4A. These fibrils display two well-protected bell-shaped regions, Ser8-Gly25 and Gly27-Val40, and a poorly protected residue, Ser26, consistent with a structural

arrangement of two β -strands connected by a turn, in agreement with a current solid-state NMR model (Figure 5A) [42]. Furthermore, the partially protected N-terminal residues, in particular Phe4 and Arg5, indicate the presence of additional secondary structure in this region. This observation is consistent with results from a limited proteolysis study, where approximately 20% of the total sample was resistant to proteolytic digest in the N-terminal region [43]. The bell-shaped protection pattern for Ser8-Gly25 and partial protection for residues Phe4 and Arg5 suggest a possible extension of the first β -strand (comprising residues 10 to 22 in the model, Figure 5A) towards the N-terminus. However, the unprotected His6 residue indicates an interruption of the secondary structure. The data therefore imply that the two residues, Phe4 and Arg5, are involved in a new structural element which forms additional intra- or inter-molecular hydrogen bonds. Residual structures in the N-terminal region of monomeric A β (1-16) and A β (1-40) have previously been identified in aqueous solution from NOE data and secondary chemical shifts [37, 44]. According to our results these structures are stabilized within the ordered environment of a fibril. The N-terminal region is known to bind divalent metal ions, such as copper and zinc, and has a propensity to form a secondary structure in which metals are coordinated by the side-chains of His6, His13, His14 and possibly Tyr10 or Glu11 [37, 45]. To verify that our results were not influenced by trace amounts of divalent metals, peptide purification and H/D exchange NMR analysis were repeated in the presence of 2 mM EDTA. The result showed virtually identical protection patterns (data not shown). The partial protection observed for the C-terminal residues of the A β (1-40) peptide, Gly37-Val40, is indicative of a less structured C-terminus. A fairly exposed C-terminus in A β (1-40) fibrils is supported by several investigations where quenched H/D exchange [26], proteolytic digests in combination with mass spectroscopy [43], proline and cysteine scanning mutagenesis [41, 46], as well as solid-state NMR study [9] were used. Overall, the protection ratios across the peptide sequence only show very little additional decay during a 24 h incubation time compared to 2 h. This is particularly true for the strongest protected residues in the β -sheet region, suggesting that they constitute a stable core of the fibril. Since the exchange rates of the amide protons may contain additional information about the intrinsic quaternary structure of the fibril, we are currently performing a detailed residue-specific analysis of the H/D exchange kinetics.

Similar to our findings, the quenched H/D exchange NMR study on A β (1-40) fibrils by Whittemore et al. [26], had also identified Gln15-Asp23 as highly, Gly37-Val40 as partially and Ser26 as poorly protected residues. However, our study identifies most N-

terminal residues prior to position 15 as partially protected, while the Whittemore study only detected two partially protected residues, Glu11 and Val12 within this region. Discrepancies are also found in the C-terminal region, comprising residues Asn27-Val36, which is well protected in our study but displays an alternating pattern with protected and exposed residues in the Wittemore study. Since the fibrils used in these studies were prepared using different solvents and agitation the most likely cause for the discrepancies is due to different preparation methods.

A direct comparison of our data on A β (1-40) and A β (1-42) fibrils is now possible since both studies were carried out using identical methods and fibril-forming conditions. AFM-analysis displayed an overall similar ultra-structural morphology, where the filament height varied between 3.5 and 7 nm due to the occurrence of laterally assembled filaments. However, while the A β (1-40) fibrils were between 100-500 nm in length the fibrils of the A β (1-42) variant often exceeded several μ m in length (Figure 1A and B). The solvent protection patterns of the two peptides showed clear discrepancies in both their N- and C-terminal regions (see Figures 4A-C). In comparison to A β (1-42), the N-terminal residues of A β (1-40), in particular Phe4 and Arg5, are significantly more protected, showing that the additional C-terminal residues, Ile41 and Val42 in A β (1-42) fibrils, affect the formation of secondary structure and possibly metal binding in the N-terminal region. A speculative explanation for the lack of protection in the N-terminal part of A β (1-42) is that the two additional residues Ile41 and Val42 interact with the N-terminal part of the first β -strand and lock it in a position so it cannot participate in the formation of additional secondary structures in the N-terminal. The C-terminal residues, Gly37-Val40, of A β (1-40) show a clear reduction of solvent protection, indicative of a more buried C-terminus in the A β (1-42) fibrils. These results are in line with previous studies where A β (1-42) fibrils, in comparison to A β (1-40) fibrils, show a higher sensitivity to proline substitutions in the C-terminal region [47]. A recent mutational analysis of the A β -sequence suggests that the main determinant for the aggregation propensity of A β (1-42) lies in the hydrophobicity of residues Ile41 and Ala42 [48]. These results support our previous suggestion that addition of the two most C-terminal residues of A β (1-42) may act as a molecular zipper between the cross- β units along the fibril axis, by adding additional hydrogen bonds to the Gly37-Ala42 structural region [31].

We mapped the solvent protection ratios in A β (1-40) fibrils onto the model in Figure 5A, the model that best agrees with our data, see Figure 6 A and B. There is a reasonable agreement also between the protection ratios for A β (1-42) fibrils [31] and the A β (1-40)

model, except for the C-terminal residues. To fully explain this protection pattern, it seems that the subunits within the A β (1-42) fibrils must shift with respect to each other as suggested in a recent solid-state NMR study (Figure 5B) [23, 24]. The protection ratios for A β (1-42) [31] mapped onto the model in Figure 5B is shown in Figure 6C and D. A shifted assembly of the filaments of A β (1-42) fibrils positions the C-terminal region of A β (1-42) in a significantly more solvent-protected environment than that of the C-terminal of A β (1-40) (cf. Figures 4A and B), creating a tightly packed hydrophobic core (Figure 6C and D). This model fully accounts for our H/D exchange NMR data on A β (1-42) fibrils [31].

In conclusion, this study presents the solvent protection pattern of A β (1-40) fibrils at a residue specific level, relates the results to current models of A β -amyloid, and compares the data with similar NMR studies, in particular our previous work on the more aggregation prone A β (1-42) variant. Most notably, the results show that the N-terminal region of A β (1-40) comprising residues Phe4-His14 is far better protected than in A β (1-42) fibrils, indicating formation of additional secondary structure in this part of the peptide. In contrast, the reduced protection of the C-terminal residues Gly37-Val40 indicates a loss of secondary structure and suggests a shift in the filament assembly.

FIGURE LEGENDS

Figure 1. Morphologies of A β (1-40) and A β (1-42) fibrils.

Tapping mode atomic force microscopy images verifying the presence of fibrillar structures after incubation of recombinant A β (1-40) and A β (1-42) peptides in 10 mM phosphate buffer pH 7.0 and 50 mM NaCl with agitation. Both images were acquired using a 5 \times 5 μ m scanning area. The scale bar in each image is 0.5 μ m. *A.* A β (1-40) fibrils with an average height of approximately 3.5-7 nm, a smooth architecture and a length between 100-500 nm. *B.* A β (1-42) fibrils with a height similar to the fibrils in *A.* A β (1-42) fibrils often exceeded several μ m in length.

Figure 2. NMR spectra of A β (1-40).

Contour plots from a selected region of a 15 N-HSQC spectrum measured on a 2 mM 15 N-labeled sample of A β (1-40). *A.* Fully protonated monomeric A β (1-40). *B* and *C.* Spectra of partly deuterated monomeric A β (1-40), recorded 11 and 203 minutes after fibril dissolution in the D₂O-solvent, respectively. Prior to dissolution, the fibrils in *B* and *C* were incubated in D₂O at pD 7.0 for two hours in order to exchange solvent-accessible protons in the fibril. Assignments are indicated in *A.*

Figure 3. Hydrogen-deuterium exchange of A β (1-40).

Examples of the measured signal decay for five amide groups within A β (1-40) as a result of post-trap exchange with the surrounding D₂O. Rings, Gln15; squares, Phe20; plus sign, Val24; diamonds, Met35; triangle, Val36.

Figure 4. Solvent protection for the backbone amide protons of A β (1-40) and A β (1-42) fibrils.

Protection is defined as the ratio of the observed intensity after a pre-incubation period in D₂O over the intensity in a completely protonated sample (defined as 100%). *A.* Solvent protection in A β (1-40) fibrils, where light and dark grey bars indicate the protection after 2 and 24 hours of pre-incubation in D₂O, respectively. *B.* Shows the solvent protection for A β (1-42) fibrils after 2 hours of pre-incubation in D₂O (the data is from ref. [31] and included for comparative reasons). *C.* A protection ratio difference plot of A β (1-40) and A β (1-42) calculated from data shown in *A* and *B.* Rings correspond to a protection ratio of 0% and crosses represent residues which exchange too fast in the monomeric state to enable

detection. Error bars show the experimental uncertainty of the measurements, determined by error propagation using standard deviations.

Figure 5. Schematic models of A β (1-40) and A β (1-42) fibrils.

Four schematic models of an A β -fibril, showing the starting point of β -strands and orientations of selected side-chains. *A.* Model of the A β (1-40) fibril derived by Petkova et al., [23]. *B.* Model of the A β (1-42) fibril built from the model in *A* together with recent solid-state NMR data on A β (1-42) fibrils by Sato et al. [24] and our H/D exchange NMR data [31]. *C.* Model of the A β (1-40) fibril proposed by Guo et al. [41]. *D.* Model of the A β (1-42) fibril derived by Lührs et al. [30].

Figure 6. Mapping of the observed protection ratios onto a fibril model.

The solvent protection ratios determined for residues within A β (1-40) and A β (1-42) fibrils are mapped onto corresponding models of the fibrils. The color code is varied between the following extremes: navy blue for complete and red for no solvent protection. Residues with no protection ratios available are depicted in grey. Main-chain hydrogen bonds are directed along the fibril axis, perpendicular to the plane of the paper. *A* and *C.* Ball and stick models showing a dimer of two cross- β units taken from a cross-section of the A β (1-40) and A β (1-42) fibril models, respectively. Assignments are indicated in some positions with their one-letter codes. *B* and *D.* Models of the fibrillar assembly for A β (1-40) and A β (1-42), respectively. The model is based on the structural model by Tycko and co-workers [23, 24], the solution structure of A β (1-16) [37], our previous study [31], and the recently proposed filament packing arrangement [24]. The image was prepared in MOLMOL [36].

ACKNOWLEDGEMENTS

We thank Dr. Robert Tycko for kindly providing us with the coordinates of the A β (9-40) amyloid model. This work was supported by Hjärnfonden, Magn. Bergvalls Foundation, Carl Trygger Foundation, Insamlingsstiftelsen Umeå Universitet, Åke Wibergs Foundation, Socialstyrelsen, Svenska Lundbecksstiftelsen, Swedish Research Science Council, patients' association FAMY-Norrbottnen, AMYL-foundation and Gustafsson Foundation.

REFERENCES

1. Pepys, M. B. (2006) Amyloidosis. *Annu. Rev. Med.* **57**, 223-241.
2. Sunde, M., Serpell, L. C., Bartlam, M., Fraser, P. E., Pepys, M. B. and Blake, C. C. (1997) Common core structure of amyloid fibrils by synchrotron X-ray diffraction. *J. Mol. Biol.* **273**, 729-739.
3. Kirschner, D. A., Abraham, C. and Selkoe, D. J. (1986) X-ray diffraction from intraneuronal paired helical filaments and extraneuronal amyloid fibers in Alzheimer disease indicates cross-beta conformation [published erratum appears in *Proc. Natl. Acad. Sci. U S A* 1986 Apr;83(8):2776]. *Proc. Natl. Acad. Sci. U S A.* **83**, 503-507.
4. Blake, C. and Serpell, L. (1996) Synchrotron X-ray studies suggest that the core of the transthyretin amyloid fibril is a continuous beta-sheet helix. *Structure.* **4**, 989-998.
5. Malinchik, S. B., Inouye, H., Szumowski, K. E. and Kirschner, D. A. (1998) Structural analysis of Alzheimer's $\beta(1-40)$ amyloid: protofilament assembly of tubular fibrils. *Biophys. J.* **74**, 537-545.
6. Pike, C. J., Burdick, D., Walencewicz, A. J., Glabe, C. G. and Cotman, C. W. (1993) Neurodegeneration induced by β -amyloid peptides in vitro: the role of peptide assembly state. *J. Neurosci.* **13**, 1676-1687.
7. Busciglio, J., Lorenzo, A. and Yankner, B. A. (1992) Methodological variables in the assessment of β amyloid neurotoxicity. *Neurobiol. Aging.* **13**, 609-612.
8. Puzzo, D. and Arancio, O. (2006) Fibrillar β -Amyloid Impairs the Late Phase of Long Term Potentiation. *Curr. Alzheimer. Res.* **3**, 179-183.
9. Petkova, A. T., Leapman, R. D., Guo, Z., Yau, W. M., Mattson, M. P. and Tycko, R. (2005) Self-propagating, molecular-level polymorphism in Alzheimer's β -amyloid fibrils. *Science.* **307**, 262-265.
10. Klein, W. L. (2002) A β toxicity in Alzheimer's disease: globular oligomers (ADDLs) as new vaccine and drug targets. *Neurochem. Int.* **41**, 345-352.
11. Wogulis, M., Wright, S., Cunningham, D., Chilcote, T., Powell, K. and Rydel, R. E. (2005) Nucleation-dependent polymerization is an essential component of amyloid-mediated neuronal cell death. *J. Neurosci.* **25**, 1071-1080.
12. Masters, C. L., Simms, G., Weinman, N. A., Multhaup, G., McDonald, B. L. and Beyreuther, K. (1985) Amyloid plaque core protein in Alzheimer disease and Down syndrome. *Proc. Natl. Acad. Sci. U S A.* **82**, 4245-4249.

13. Shinkai, Y., Yoshimura, M., Ito, Y., Odaka, A., Suzuki, N., Yanagisawa, K. and Ihara, Y. (1995) Amyloid β -proteins 1-40 and 1-42(43) in the soluble fraction of extra- and intracranial blood vessels. *Ann. Neurol.* **38**, 421-428
14. Iwatsubo, T., Odaka, A., Suzuki, N., Mizusawa, H., Nukina, N. and Ihara, Y. (1994) Visualization of A β 42(43) and A β 40 in senile plaques with end-specific A β monoclonals: evidence that an initially deposited species is A β 42(43). *Neuron.* **13**, 45-53.
15. Lemere, C. A., Blusztajn, J. K., Yamaguchi, H., Wisniewski, T., Saido, T. C. and Selkoe, D. J. (1996) Sequence of deposition of heterogeneous amyloid β -peptides and APO E in Down syndrome: implications for initial events in amyloid plaque formation. *Neurobiol. Dis.* **3**, 16-32.
16. Suzuki, N., Cheung, T. T., Cai, X. D., Odaka, A., Otvos, L., Jr., Eckman, C., Golde, T. E. and Younkin, S. G. (1994) An increased percentage of long amyloid β protein secreted by familial amyloid β protein precursor (β APP717) mutants. *Science.* **264**, 1336-1340.
17. Eckman, C. B., Mehta, N. D., Crook, R., Perez-tur, J., Prihar, G., Pfeiffer, E., Graff-Radford, N., Hinder, P., Yager, D., Zenk, B., Refolo, L. M., Prada, C. M., Younkin, S. G., Hutton, M. and Hardy, J. (1997) A new pathogenic mutation in the APP gene (I716V) increases the relative proportion of A β 42(43). *Hum. Mol. Genet.* **6**, 2087-2089.
18. McGowan, E., Pickford, F., Kim, J., Onstead, L., Eriksen, J., Yu, C., Skipper, L., Murphy, M. P., Beard, J., Das, P., Jansen, K., Delucia, M., Lin, W. L., Dolios, G., Wang, R., Eckman, C. B., Dickson, D. W., Hutton, M., Hardy, J. and Golde, T. (2005) A β 42 is essential for parenchymal and vascular amyloid deposition in mice. *Neuron.* **47**, 191-199.
19. Petkova, A. T., Ishii, Y., Balbach, J. J., Antzutkin, O. N., Leapman, R. D., Delaglio, F. and Tycko, R. (2002) A structural model for Alzheimer's β -amyloid fibrils based on experimental constraints from solid state NMR. *Proc. Natl. Acad. Sci. U S A.* **99**, 16742-16747.
20. Benzinger, T. L., Gregory, D. M., Burkoth, T. S., Miller-Auer, H., Lynn, D. G., Botto, R. E. and Meredith, S. C. (2000) Two-dimensional structure of β -amyloid(10-35) fibrils. *Biochemistry.* **39**, 3491-3499.
21. Antzutkin, O. N., Leapman, R. D., Balbach, J. J. and Tycko, R. (2002) Supramolecular structural constraints on Alzheimer's β -amyloid fibrils from electron microscopy and solid-state nuclear magnetic resonance. *Biochemistry.* **41**, 15436-15450.

22. Balbach, J. J., Petkova, A. T., Oyler, N. A., Antzutkin, O. N., Gordon, D. J., Meredith, S. C. and Tycko, R. (2002) Supramolecular structure in full-length Alzheimer's β -amyloid fibrils: evidence for a parallel β -sheet organization from solid-state nuclear magnetic resonance. *Biophys. J.* **83**, 1205-1216.
23. Petkova, A. T., Yau, W. M. and Tycko, R. (2006) Experimental constraints on quaternary structure in Alzheimer's β -amyloid fibrils. *Biochemistry.* **45**, 498-512.
24. Sato, T., Kienlen-Campard, P., Ahmed, M., Liu, W., Li, H., Elliott, J. I., Aimoto, S., Constantinescu, S. N., Octave, J. N. and Smith, S. O. (2006) Inhibitors of amyloid toxicity based on β -sheet packing of A β 40 and A β 42. *Biochemistry.* **45**, 5503-5516.
25. Alexandrescu, A. T. (2001) An NMR-based quenched hydrogen exchange investigation of model amyloid fibrils formed by cold shock protein A. *Pac. Symp. Biocomput.*, 67-78.
26. Whittemore, N. A., Mishra, R., Kheterpal, I., Williams, A. D., Wetzel, R. and Serpersu, E. H. (2005) Hydrogen-deuterium (H/D) exchange mapping of A β 1-40 amyloid fibril secondary structure using nuclear magnetic resonance spectroscopy. *Biochemistry.* **44**, 4434-4441.
27. Olofsson, A., Ippel, J. H., Wijmenga, S. S., Lundgren, E. and Öhman, A. (2004) Probing solvent accessibility of transthyretin amyloid by solution NMR spectroscopy. *J. Biol. Chem.* **279**, 5699-5707.
28. Ippel, J. H., Olofsson, A., Schleucher, J., Lundgren, E. and Wijmenga, S. S. (2002) Probing solvent accessibility of amyloid fibrils by solution NMR spectroscopy. *Proc. Natl. Acad. Sci. U S A.* **99**, 8648-8653.
29. Hoshino, M., Katou, H., Hagihara, Y., Hasegawa, K., Naiki, H. and Goto, Y. (2002) Mapping the core of the beta(2)-microglobulin amyloid fibril by H/D exchange. *Nat. Struct. Biol.* **9**, 332-336.
30. Lührs, T., Ritter, C., Adrian, M., Riek-Loher, D., Bohrmann, B., Döbeli, H., Schubert, D. and Riek, R. (2005) 3D structure of Alzheimer's amyloid- β (1-42) fibrils. *Proc. Natl. Acad. Sci. U S A.* **102**, 17342-17347.
31. Olofsson, A., Sauer-Eriksson, A. E. and Öhman, A. (2006) The solvent protection of alzheimer amyloid- β -(1-42) fibrils as determined by solution NMR spectroscopy. *J. Biol. Chem.* **281**, 477-483.
32. Delaglio, F., Grzesiek, S., Vuister, G. W., Zhu, G., Pfeifer, J. and Bax, A. (1995) NMRPipe: a multidimensional spectral processing system based on UNIX pipes. *J. Biomol. NMR.* **6**, 277-293.

33. Helgstrand, M., Kraulis, P., Allard, P. and Härd, T. (2000) Ansig for Windows: an interactive computer program for semiautomatic assignment of protein NMR spectra. *J. Biomol. NMR.* **18**, 329-336.
34. Crescenzi, O., Tomaselli, S., Guerrini, R., Salvadori, S., D'Ursi, A. M., Temussi, P. A. and Picone, D. (2002) Solution structure of the Alzheimer amyloid β -peptide (1-42) in an apolar microenvironment. Similarity with a virus fusion domain. *Eur. J. Biochem.* **269**, 5642-5648.
35. Johnson, B.A. and Blevins, R.A. (1994) NMRView: A computer program for the visualization and analysis of NMR data. *J. Biomol. NMR.* **4**, 603-614.
36. Koradi, R., Billeter, M. and Wüthrich, K. (1996) MOLMOL: a program for display and analysis of macromolecular structures. *J. Mol. Graph.* **14**, 51-55, 29-32.
37. Zirah, S., Kozin, S. A., Mazur, A. K., Blond, A., Cheminant, M., Segalas-Milazzo, I., Debey, P. and Rebuffat, S. (2006) Structural changes of region 1-16 of the Alzheimer disease amyloid β -peptide upon zinc binding and in vitro aging. *J. Biol. Chem.* **281**, 2151-2161.
38. Guex, N. and Peitsch, M. C. (1997) SWISS-MODEL and the Swiss-PdbViewer: an environment for comparative protein modeling. *Electrophoresis.* **18**, 2714-2723.
39. Tycko, R. (2006) Molecular structure of amyloid fibrils: insights from solid-state NMR. *Q. Rev. Biophys.*, 1-55.
40. Morgan, C., Colombres, M., Nunez, M. T. and Inestrosa, N. C. (2004) Structure and function of amyloid in Alzheimer's disease. *Prog. Neurobiol.* **74**, 323-349.
41. Shivaprasad, S. and Wetzel, R. (2006) Scanning cysteine mutagenesis analysis of A β -(1-40) amyloid fibrils. *J. Biol. Chem.* **281**, 993-1000.
42. Paravastu, A. K., Petkova, A. T. and Tycko, R. (2006) Polymorphic Fibril Formation by Residues 10-40 of the Alzheimer's β -Amyloid Peptide. *Biophys. J.* **90**, 4618-4629.
43. Kheterpal, I., Williams, A., Murphy, C., Bledsoe, B. and Wetzel, R. (2001) Structural features of the A β amyloid fibril elucidated by limited proteolysis. *Biochemistry.* **40**, 11757-11767.
44. Riek, R., Güntert, P., Döbeli, H., Wipf, B. and Wüthrich, K. (2001) NMR studies in aqueous solution fail to identify significant conformational differences between the monomeric forms of two Alzheimer peptides with widely different plaque-competence, A β (1-40)(ox) and A β (1-42)(ox). *Eur. J. Biochem.* **268**, 5930-5936.

45. Smith, D. P., Smith, D. G., Curtain, C. C., Boas, J. F., Pilbrow, J. R., Ciccotosto, G. D., Lau, T. L., Tew, D. J., Perez, K., Wade, J. D., Bush, A. I., Drew, S. C., Separovic, F., Masters, C. L., Cappai, R. and Barnham, K. J. (2006) Copper-mediated amyloid- β toxicity is associated with an intermolecular histidine bridge. *J. Biol. Chem.* **281**, 15145-15154.
46. Williams, A. D., Portelius, E., Kheterpal, I., Guo, J. T., Cook, K. D., Xu, Y. and Wetzel, R. (2004) Mapping A β amyloid fibril secondary structure using scanning proline mutagenesis. *J. Mol. Biol.* **335**, 833-842.
47. Morimoto, A., Irie, K., Murakami, K., Masuda, Y., Ohigashi, H., Nagao, M., Fukuda, H., Shimizu, T. and Shirasawa, T. (2004) Analysis of the secondary structure of β -amyloid (A β 42) fibrils by systematic proline replacement. *J. Biol. Chem.* **279**, 52781-52788.
48. Kim, W. and Hecht, M. H. (2005) Sequence determinants of enhanced amyloidogenicity of Alzheimer A β 42 peptide relative to A β 40. *J. Biol. Chem.* **280**, 35069-35076.

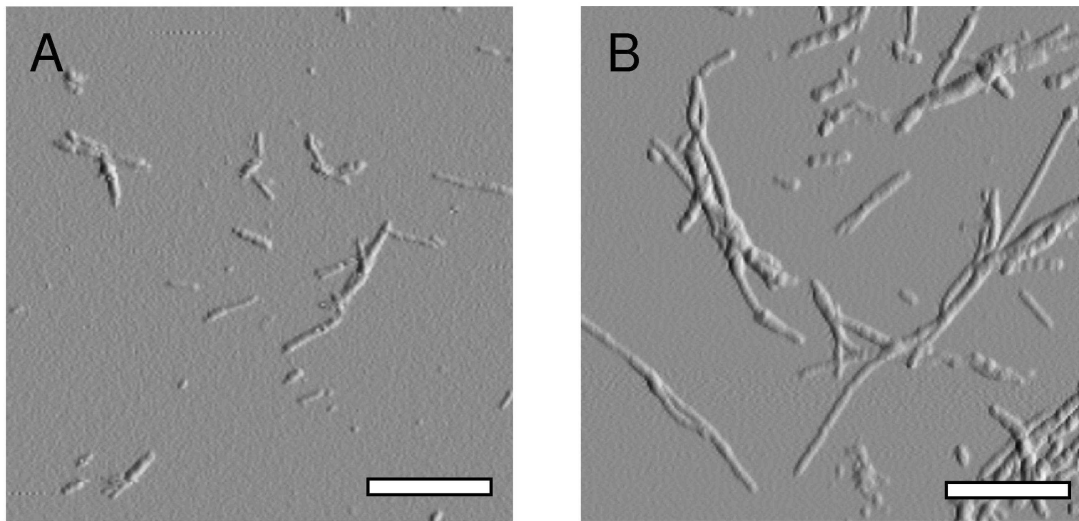


Figure 1.

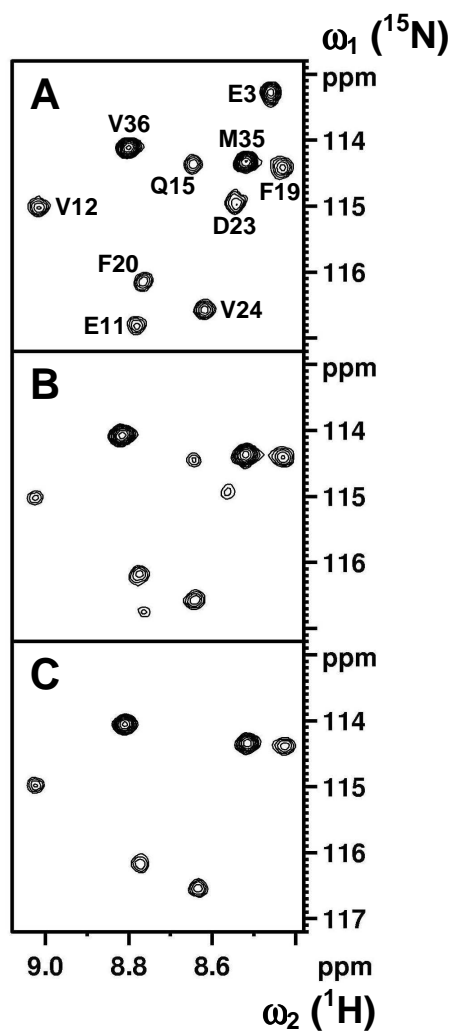


Figure 2.

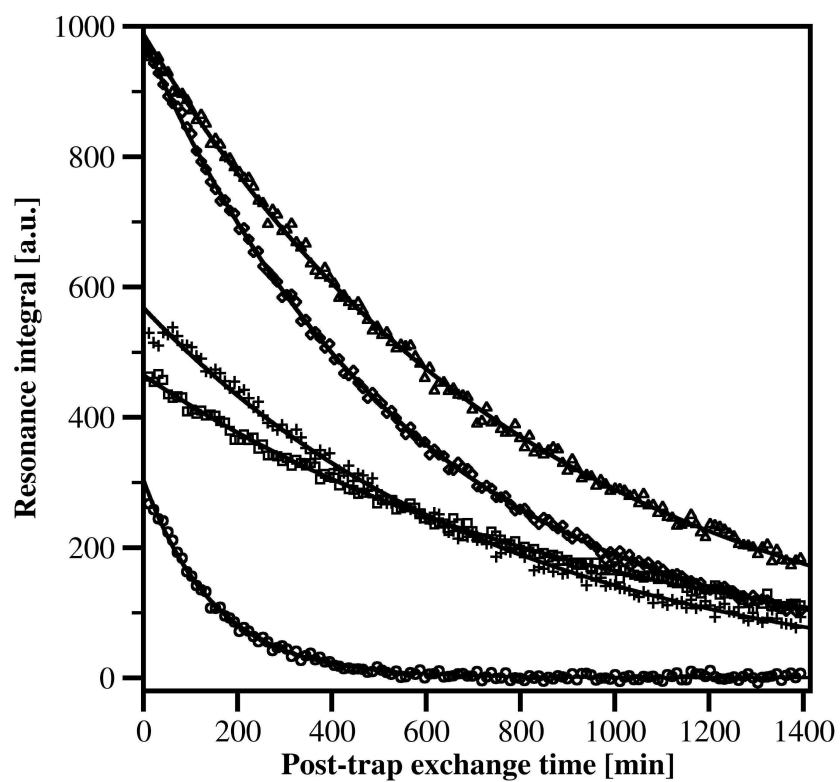


Figure 3.

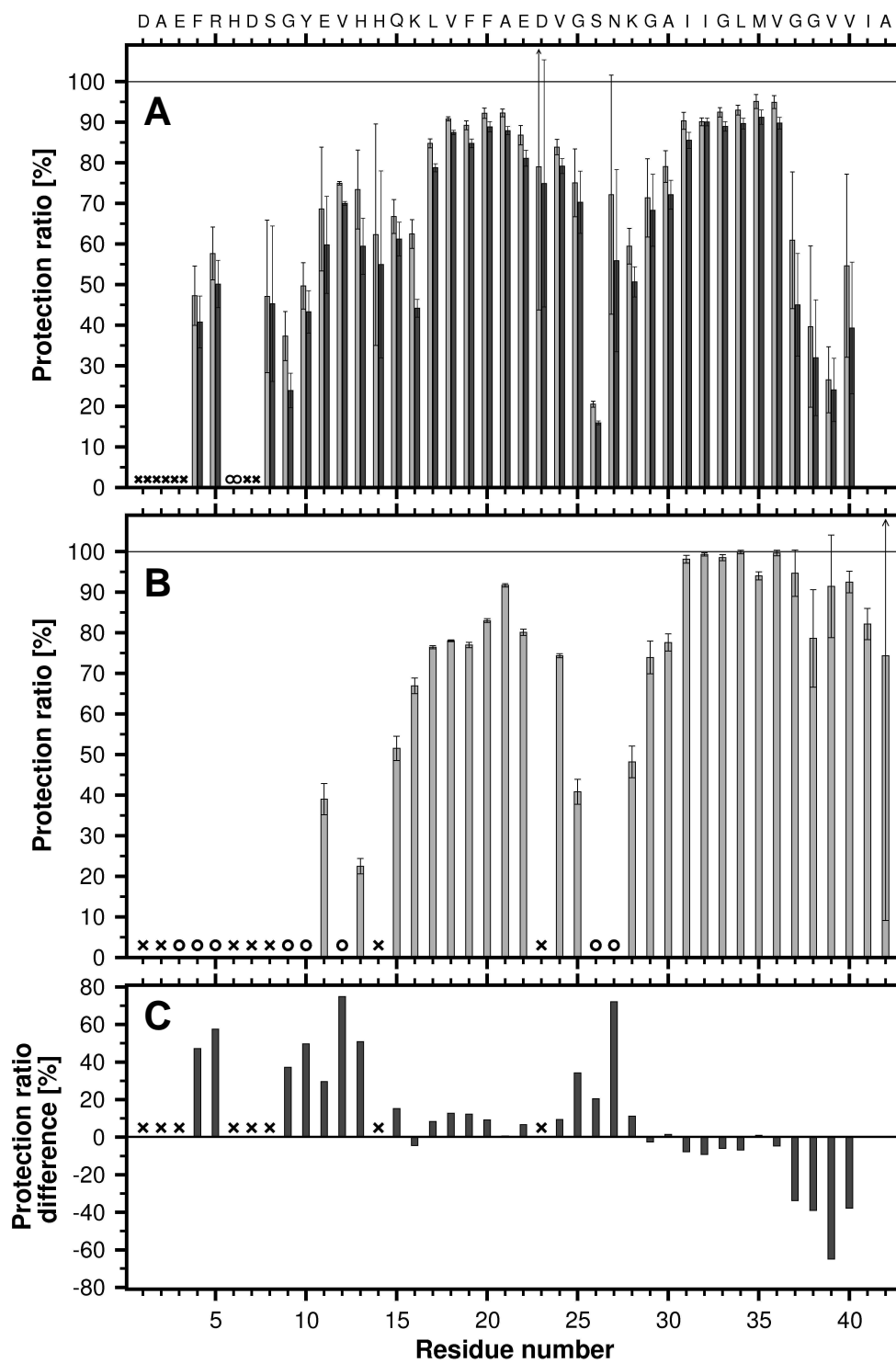


Figure 4.

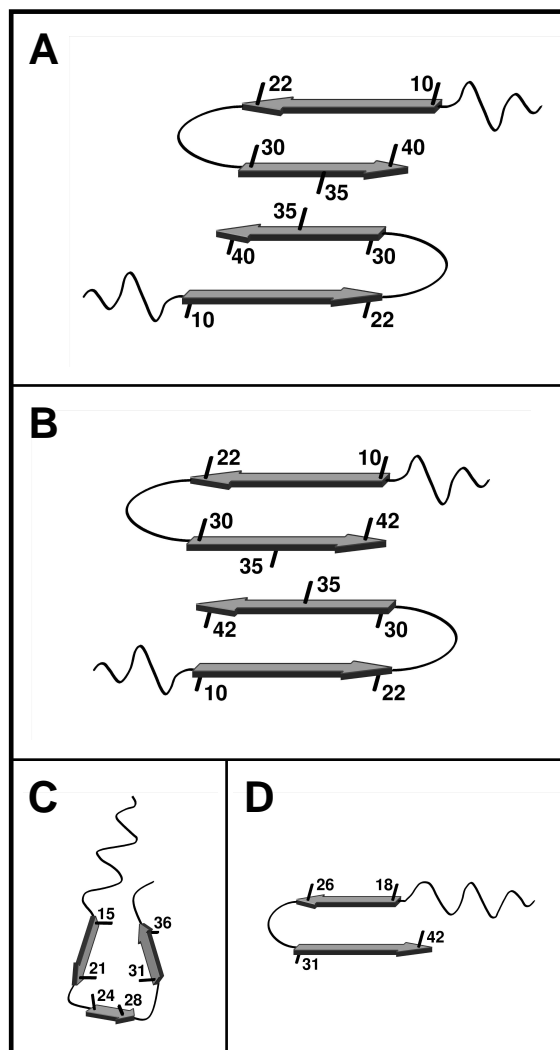


Figure 5.

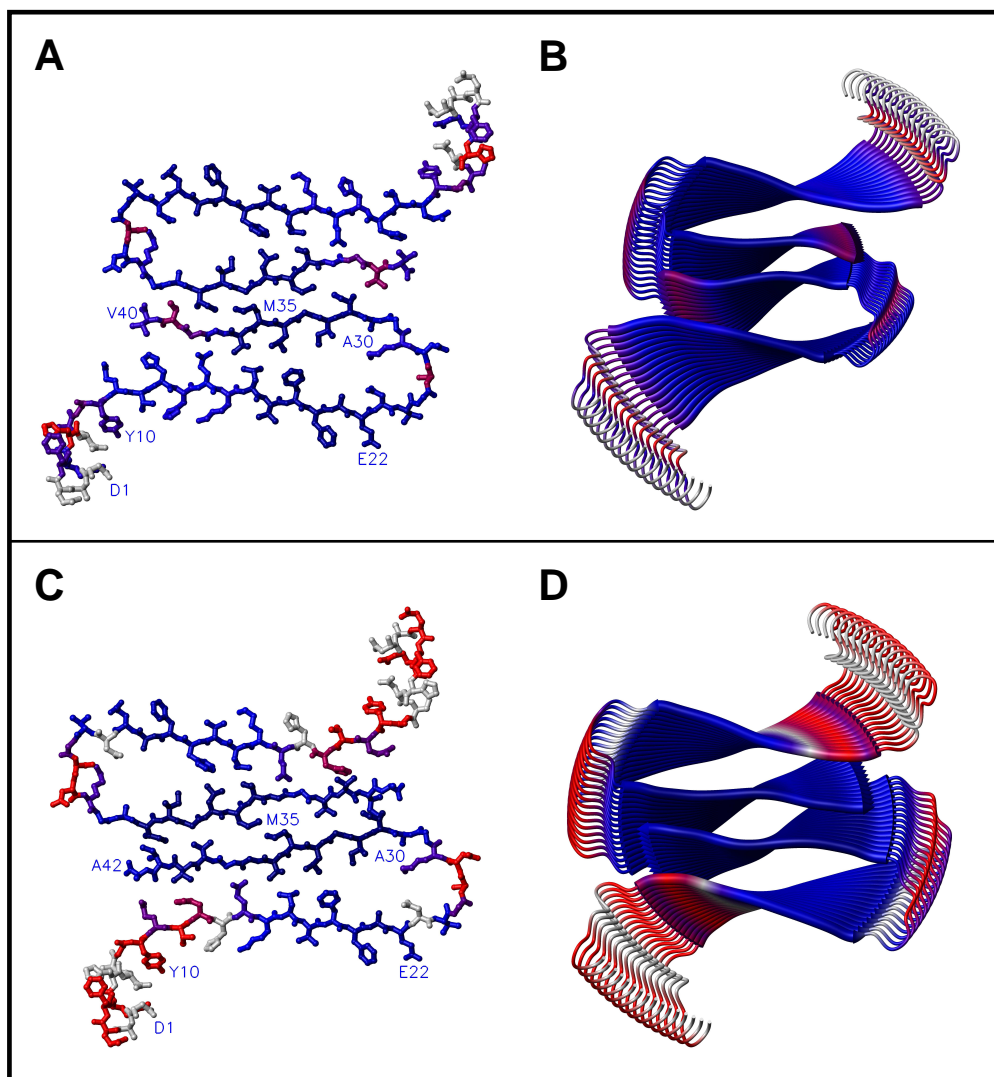


Figure 6.